A METHOD TO ESTIMATE FRIED'S SEEING PARAMETER FROM A TIME SERIES OF ARBITRARY RESOLVED STRUCTURES IMAGED THROUGH THE ATMOSPHERE

O. von der Lühe
Kiepenheuer-Institut für Sonnenphysik
Freiburg, Schöneckstr. 6, W.- Germany

Abstract

One of the major fields of application of speckle-interferometric and speckle-imaging techniques is the photometry of astronomical objects exhibiting structure smaller than the seeing limit. The accuracy of the photometry depends critically on the accuracy to which the modulation transfer function (MTF), that describes the atmospheric-telescopic attenuation of the Fourier amplitudes of the object under consideration, is known. The estimation of the effective MTF is especially difficult when no known reference object is within the field of view.

A method is presented that allows to estimate the effective MTF from the observation of arbitrary structure with the use of FRIED-KORFF theory. The ratio of the squared modulus of the average Fourier transform and the average power spectrum serves as an estimator for the FRIED parameter r_o. To a first approximation, this ratio is independent from the observed object. Additionally, the behaviour of the ratio in regions beyond the seeing limit in the Fourier plane may be analyzed to obtain an estimate of the speckle interferometry signal-to-noise ratio. The basic concept of the ratio method will be described, its accuracy will be discussed. First results on the application of the ratio method to observations of solar granulation will be presented.

I. Introduction

When applying speckle interferometric and speckle imaging techniques to astronomical observations, it is important to know the effective modulation transfer function (MTF) of the combined system of the atmosphere and the telescope. In nighttime speckle interferometry, the usual procedure is to observe a near-by unresolvable star as a reference simultaneously with the object under consideration, so the MTF can be estimated from the average power spectrum of the reference object.

The situation becomes more complicated when no suitable reference object exists within the field of view. In particular, this is the case when small scale

Proceedings of the IAU Colloquium No. 79: "Very Large Telescopes, their Instrumentation and Programs", Garching, April 9–12, 1984.

structure on the solar surface is observed. The shape of the structure is inherently unknown and typical lifetimes of small scale intensity fluctuations in the solar photosphere range from a few minutes to the order of half an hour. Here general assumptions on the shape of the average MTF are necessary. In speckle imaging (NOYES et al., 1981) for example, advantage was taken of the conception that the averaged squared modulus of the optical transfer function (OTF) consists of a strong low frequency term that describes the average MTF and a weak term proportional to the OTF of a diffraction limited telescope (DAINTY, 1974).

Another method, devoted to solar observations, has been discussed by AIME et al. (1978). Here, the power spectra of two observations of the same structure are compared, their ratio being independent from the object spectrum. From the shape of the observed ratio, the corresponding values of FRIED's (1966) seeing parameter r_o are derived by comparison with theoretical ratios obtained with KORFF's (1973) theory. However, r_o estimates thus obtained would be very uncertain when the difference between the two r_o values were small.

Here, a different method to obtain r_o from a time series of observations is presented (sect. II). The method takes advantage of the differences between the average observed Fourier transform and the average power spectrum. The object spectrum is eliminated by computing the ratio of the squared modulus of the average Fourier transform and the average power spectrum. From the quantity thus obtained, the corresponding r_o is inferred and used to construct the appropriate KORFF modulation transfer function. Additionally, closer examination of the ratio allows to estimate the signal-to-noise ratio of the speckle interferometry signal in the average power spectrum. The results of test experiments are presented in sect. III.

II. Theory

II.1. The basis of the spectral ratio method

Consider a time series of N short-exposure-time pictures $I_1(\vec{x}) \ldots, I_N(\vec{x})$ of a temporarily stable, but otherwise arbitrary, small scale structure imaged through the atmosphere. $\vec{x}$ is the spatial coordinate in the telescope focal plane. The term "small scale" refers to the property of the observed object $I_o(\vec{x})$ to actually contain structure with scales smaller than the seeing limit. When imaging occurs under isoplanatic conditions, the Fourier transform $F_i(\vec{s})$ of the i-th observation can be written as:

https://doi.org/10.1017/S0252921100108401 Published online by Cambridge University Press

$$F_i(\bar{s}) = F_o(\bar{s}) \cdot S_i(\bar{s}) \qquad (1)$$

Here, $\bar{s}$ is the spatial wave number coordinate, $F_o(\bar{s})$ is the object Fourier transform and $S_i(\bar{s})$ is the effective Optical transfer function (OTF) of atmosphere and telescope, when picture I_i was taken.

It is convenient to express quantities in the Fourier domain as functions of the "relative wave number" coordinate $\bar{q}$, which is defined by:

$$\bar{q} := \bar{s}/s_c \quad ; \quad s_c = \frac{D}{\lambda \cdot f} \quad ; \quad q := |\bar{q}|$$

Here, s_c is the theoretical cutoff of a telescope with entrance pupil diameter D and effective focal length f, when observations were taken at light wavelength λ. Thus, within the resolution limit of the telescope, the modulus of $\bar{q}$ varies between 0 and 1.

In Speckle Interferometry, averages of Fourier quantities are evaluated, and the objective here is to obtain an expression from eqn. (1) that is as independent as possible from the object spectrum F_o. Let $\langle \cdot \rangle$ denote arithmetic averaging and define

$$\varepsilon(\bar{q}) := \frac{|\langle F_i(\bar{q})\rangle|^2}{\langle |F_i(\bar{q})|^2\rangle} = \frac{|F_o(\bar{q})|^2}{|F_o(\bar{q})|^2} \cdot \frac{|\langle S_i(\bar{q})\rangle|^2}{\langle |S_i(\bar{q})|^2\rangle} \qquad (2)$$

The numerator of the left-hand side of eqn. (2)is the squared modulus of the average observed Fourier transform, while the denominator is the average observed power spectrum. If $F_o(q)$ is non zero for all $\bar{q}$, i.e. I_o really is a "small scale" object, eqn. (2) turns to:

$$\varepsilon(\bar{q}) = \frac{|\langle S_i(\bar{q})\rangle|^2}{\langle |S_i(\bar{q})|^2\rangle} \qquad (3)$$

The use of the expression (3) was motivated by the following consideration: in classical speckle interferometry, the averaged squared modulus of the OTF is believed to be finite in the whole range $0 < q < 1$ while $\langle S_i(q)\rangle$ quickly tends towards zero for q larger than the atmospheric cutoff q_a. Within FRIED's and KORFF's theories, q_a is approximately related to FRIED's parameter r_o by $q_a \sim \frac{r_o}{D}$. Thus, the evaluation of $\varepsilon(\bar{q})$ may allow the estimation of r_o. In the following, $\varepsilon(\bar{q})$ will be referred to as "Spectral ratio".

The results of FRIED (1966) and KORFF (1973) were taken to calculate the expected profile of $\varepsilon(\bar{q})$. Under ergodic conditions, both $\langle S_i(\bar{q})\rangle$ and $|\langle S_i(\bar{q})\rangle|^2$ should be isotropic and thus they should be merely functions of the wave number modulus q.

https://doi.org/10.1017/S0252921100108401 Published online by Cambridge University Press

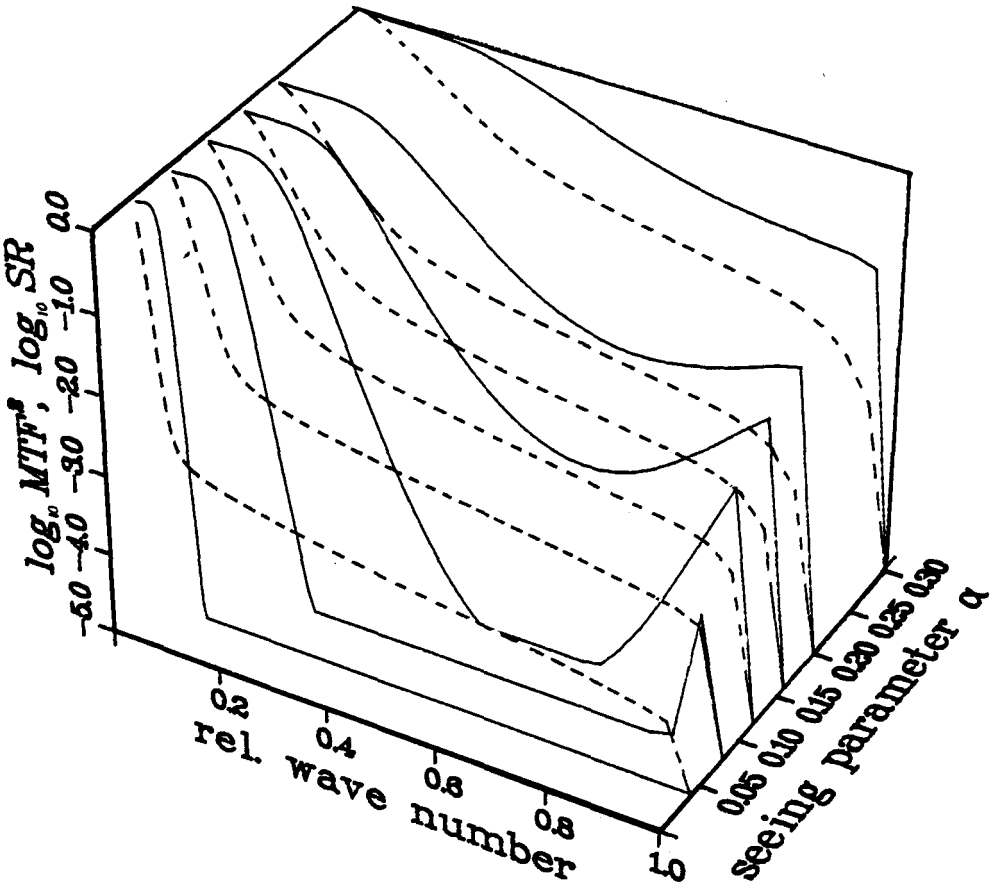

Fig.1. Spectral ratio profiles as expected from the ratio of FRIED's and KORFF's average modulation transfer functions (solid curves) amd the corresponding KORFF MTF^2 curves (dashed). Each curve is displayed as a function of the spatial relative wave number $q = s / s_c$, where $s_c = \lambda/D$ is the cutoff wave number of the telescope with entrance pupil diameter D. The curve parameter is the modified FRIED seeing parameter $\alpha = r_o/D$. The increase of the spectral ratios close to q = 1 is an artifact and is caused by a possible deficiency in FRIED's theory of an average short-exposure-time MTF.

https://doi.org/10.1017/S0252921100108401 Published online by Cambridge University Press

In the theoretical calculations, the "near-field" case, short exposure times and an unobscured, circular entrance pupil were assumed. Defining the "modified FRIED parameter" $\alpha = \frac{r_o}{D}$, theoretical spectral ratio profiles were calculated from different α values ranging from o.o4 to o.3o. The results are presented in Fig.1. The solid curves represent the expected profile of $\mathcal{E}$ as a function of q and α, while the dashed curves represent the corresponding KORFF modulation transfer functions.

II.2. The influence of noise

In all practical cases, the Fourier quantities in eq.(2) are affected by noise. Some additional considerations allow to use the spectral ratio as an estimator for the speckle interferometry signal-to-noise ratio.

Consider an additive noise term $R_i(q)$ in the Fourier plane; eqn. (1) changes to

$$F_i(\bar{q}) = F_0(\bar{q}) \cdot S_i(\bar{q}) + R_i(\bar{q}) \tag{4}$$

If the frame number N is high enough to ensure that averages of $S_i(\bar{q})$ and $|S_i(\bar{q})|^2$ are well represented by their ensemble averages, then the spectral ratio $\mathcal{E}(\bar{q})$ can be represented by

$$\mathcal{E}(\bar{q})\Big|_{q>\alpha} = \frac{|\langle R_i(\bar{q})\rangle|^2}{|F_0(\bar{q})|^2 \cdot \langle|S_i(\bar{q})|^2\rangle + \langle|R_i(\bar{q})|^2\rangle} \tag{5}$$

in the region beyond the seeing limit, i.e. the region where $\langle S_i(\bar{q})\rangle$ is essentially zero.

In order to evaluate eqn. (5), one has to make assumptions on the statistical properties of $R_i(\bar{q})$. If we assume that $R_i(\bar{q})$ is a random, normally distributed complex variable with zero mean and variance $\sigma^2 = \sigma^2_{REAL} + \sigma^2_{IMAG}$, then $|\langle R_i(\bar{q})\rangle|^2$ is exponentially distributed with mean σ^2/N and variance $2\,\sigma^4/N^2$ while $\langle |R_i(\bar{q})|^2\rangle$ follows a χ^2-distribution with mean σ^2 and variance $\sigma^4/N-1$.

With this model, it is possible to obtain an estimate of the signal-to-noise ratio in the classical speckle regions in the Fourier domain. All that is needed is an estimate of σ^2, which can be obtained by analysing flat field frames or uniformly exposed photographs. If $G_j(\bar{q})$ represent the Fourier transforms of such a series, preferably having the same amount of frames N, then we expect $\langle |G_j(\bar{q})|^2\rangle$ to be an estimate of σ^2. Now, eqn (2) is slightly modified

https://doi.org/10.1017/S0252921100108401 Published online by Cambridge University Press

to: $$\varepsilon^*(\bar{q}) := \frac{|\langle F_i(\bar{q})\rangle|^2}{\langle|F_i(\bar{q})|^2\rangle - \langle|G_j(\bar{q})|^2\rangle} \tag{6}$$

When the noise bias in the average power spectrum is subtracted, a residual error remains that has a standard deviation of $\sigma^2/(N-1)^{1/2}$ within the Gaussian noise model. Defining the signal-to-noise ratio SNR

$$SNR = \frac{|F_0(\bar{q})|^2 \cdot \langle|S_i(\bar{q})|^2\rangle}{\sigma^2/\sqrt{N-1}} \tag{7}$$

and assuming that SNR is high, we obtain for the expectation of ε^* in the region beyond the seeing limit (E $\langle\cdot\rangle$ denotes the expected value):

$$E\left[\varepsilon^*(\bar{q})/_{q>\alpha}\right] = \frac{\sigma^2}{N \cdot |F_0(\bar{q})|^2 \langle|S_i(\bar{q})|^2\rangle} \tag{8}$$

or, inserting eqn. (8) into eqn. (7):

$$SNR = \frac{\sqrt{N-1}}{N} \cdot \frac{1}{\varepsilon^*(\bar{q})/_{q>\alpha}} \tag{9}$$

Equation (9) has to be understood as follows: If we observe a typical value for the modified spectral ratio ε^* in a region beyond the seeing limit ($q > \alpha$), we would expect the SNR to be as large as the result of eqn. (9). The significance of this statement will be discussed in the next section.

For the regions in the Fourier plane where SNR is small, we can neglect the signal $|F_0(\bar{q})|^2 \langle|S_i(\bar{q})|^2\rangle$. Thus, eqn. (6) turns to

$$\varepsilon^*(\bar{q})/_{\text{NO SIGNAL}} = \frac{|\langle R_i(\bar{q})\rangle|^2}{\langle|R_i(\bar{q})|^2\rangle - E[\langle|R_i(\bar{q})|^2\rangle]} \tag{10}$$

Within the gaussian noise model, a random variable with mean σ^2/N is divided by a random variable with zero mean, which approximately follows a gaussian distribution when N is fairly large. The numerator is always positive while the denominator might be positive or negative, so observed values of $\varepsilon^*(\bar{q})$ might be negative in this region. Moreover, values of ε that have moduli considerably larger than unity are very likely. Thus domains with a small SNR in the Fourier plane would exhibit a conspicuous, chaotic appearance.

Another practically relevant case is the presence of a deterministic noise term in the Fourier transforms. Terms like these occur frequently when modern diode matrix arrays are used as detectors; they are often called "fixed-pattern" noise. Consi-

https://doi.org/10.1017/S0252921100108401 Published online by Cambridge University Press

der an additive, systematic component $R_s(\bar{q})$ in the observed Fourier transform that is independent from $S_i(\bar{q})$ and is identical for all frames i = 1,...,N:

$$F_i(\bar{q}) = F_0(\bar{q}) \cdot S_i(\bar{q}) + R_s(\bar{q}) \tag{11}$$

Inserting eqn. (11) into eqn. (2) yields for the region beyond the seeing limit:

$$\varepsilon(\bar{q})\big|_{q>\alpha} = \frac{|R_s(\bar{q})|^2}{|F_0(\bar{q})|^2 \cdot \langle |S_i(\bar{q})|^2 \rangle + |R_s(\bar{q})|^2} \tag{12}$$

In this case, the SNR is defined by:

$$SNR = \frac{|F_0(\bar{q})|^2 \cdot \langle |S_i(\bar{q})|^2 \rangle}{|R_s(\bar{q})|^2} \tag{13}$$

From eqn. (12), we get:

$$SNR = \frac{1}{\varepsilon(\bar{q})\big|_{q>\alpha}} - 1 \tag{14}$$

Let us summarize the essence of this section:

- The spectral ratio as defined in eqns. (3) and (6) may serve as an estimator for the FRIED parameter $\alpha = \frac{r_0}{D}$, that is independent from the object being observed. The only requirement posed upon the observed structure is that there exists a signal beyond the seeing limit $q > \alpha$. The parameter α may be estimated by analysing the decrease of the spectral ratio at small spatial wave numbers; α, in turn, may be used to calculate a theoretical MTF in order to recalibrate Fourier amplitudes.

- In the region beyond the seeing limit, the spectral ratio may be used as an estimator of the speckle interferometry signal-to-noise ratio in the average power spectrum. The presence of a region where the spectral ratio is small and decreases when the frame number N is increased, indicates the presence of a random noise component and eqn. (9) may be used to estimate the signal-to-noise ratio. A region where the spectral ratio exhibits chaotic behaviour indicates the absence of signal. When the ratio is independent from the frame number it can be assumed that a systematic noise component is present in the Fourier data.

https://doi.org/10.1017/S0252921100108401 Published online by Cambridge University Press

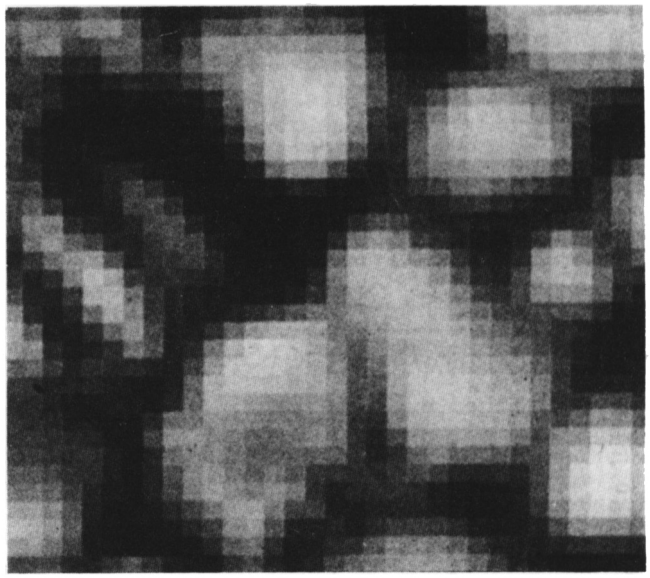

Fig.2. A sample frame from the data analysed in experiment 1. The field of view covers 6".23x6".23 of solar granulation near the disk center. The elongation of this picture is artificial.

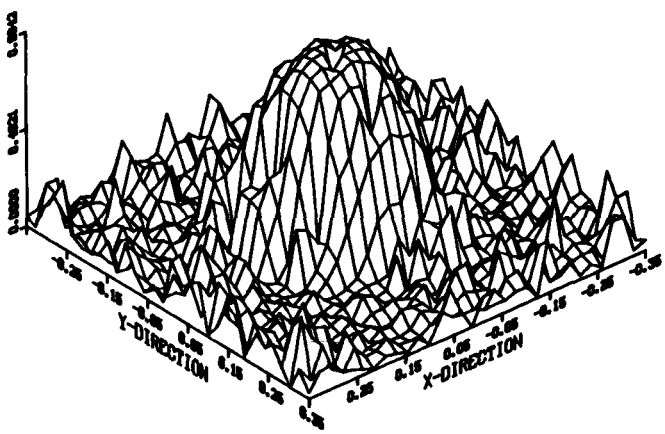

Fig.3. The 2D spectral ratio obtained from the first data set in experiment 1, displayed as a surface plot. The horizontal units are relative wave numbers, the vertical scale ranges from o.oo to o.98.

https://doi.org/10.1017/S0252921100108401 Published online by Cambridge University Press

III. Experiments

The spectral ratio method has been developed with regard to Speckle interferometry of solar small scale structure. Here, we report on some observations and their analysis, in order to demonstrate the performance of the method.

Firstly, granulation near to the center of the solar disk was observed with a 32 by 32 diode matrix array at Sacramento Peak Observatory tower telescope. A technical description of the data is given in table I. Five consecutive time series, 255 frames each, covering 75 seconds of time altogether, were analyzed. After compensation of dark current and gain table, the average intensity and the average gradient was removed from each individual frame by means of a bi-linear least-squares fit. After applying a cosine apodisation bell, the frames were Fourier transformed and the spectral ratio was calculated. An analysis of the random noise contributions was performed by treating a run on defocused sunlight in exactly the same way.

Fig.2 shows a sample frame from the first time series. Fig. 3 shows the two-dimensional spectral ratio obtained from the first time series. It is observed that all two-dimensional spectral ratios are radially symmetric, so azimuthal averages about zero spatial wave number may be calculated. Turning from cartesian coordinates (q_1, q_2) to polar coordinates (q, ϑ) in the Fourier plane, the "radial spectral ratio" $\varepsilon_r(q)$ is defined by:

$$\varepsilon_r(q) = \frac{1}{2\pi q} \int_0^{2\pi} \varepsilon(q, \vartheta)\, d\vartheta \qquad (15)$$

Fig.4 presents the radial spectral ratios for all five time series. In Fig.5, the observed radial spectral ratios are compared with the theoretical radial spectral ratio profiles as expected from FRIED's and KORFF's theoretical modulation transfer functions. From this comparison, the appropriate α values for each set was derived. In Table II, the values for α thus found are listed together with the corresponding FRIED parameter r_o, the rms image motion and the observed ("raw") rms contrast obtained from the average power spectra. It was observed that the noise level in the high frequency region of approx. o.o7 is independent from the number N of the frames analysed. Therefore, we assume that this level originates from a systematic noise component in the Fourier transforms. The α inferences were used to construct the appropriate KORFF MTF in order to recalibrate the average power spectra. The raw and compensated radial power spectra are presented in Fig.6. If $P(q, \vartheta)$ is the two-dimensional power spectrum, the radial power spectrum is defined by

https://doi.org/10.1017/S0252921100108401 Published online by Cambridge University Press

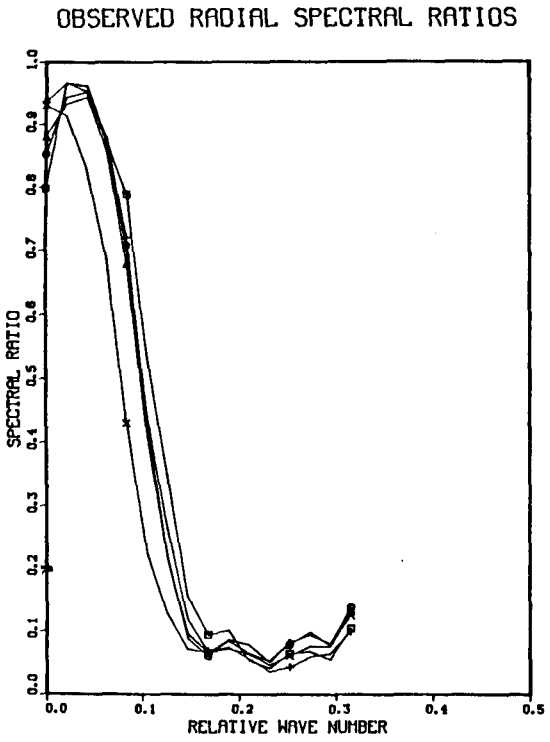

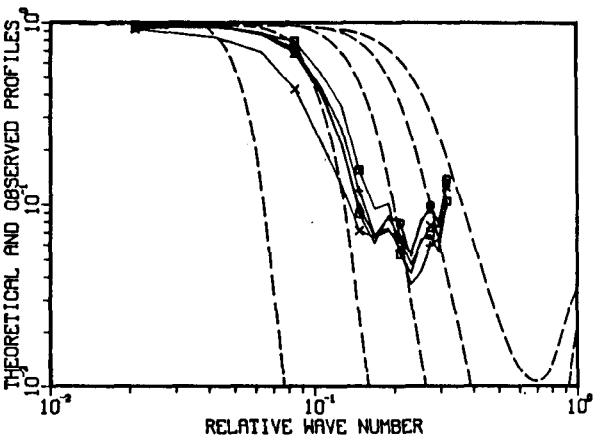

Fig.4. (left)
The azimuthal average of the spectral ratios obtained from all five data sets in experiment 1. The differences in the decay of the curves reflect the differences in seeing conditions during observation.

Fig.5. (above)
The same spectral ratio profiles as in fig.4 (solid lines), in comparison with the spectral ratio as expected from FRIED/KORFF theorv (see also Fig.1; dashed lines). The dashed lines correspond to α values of (from left to right): o.o4, o.o8, o.12, o.16, o.2o.

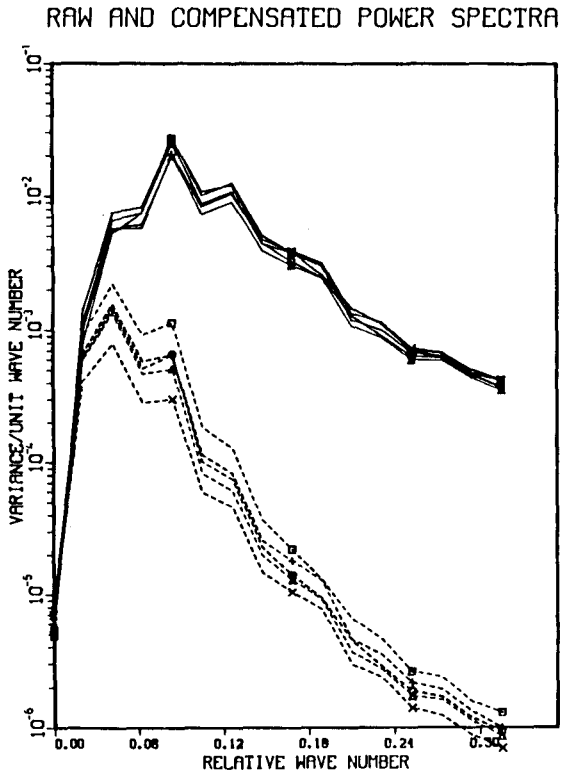

Fig.6. (left)
Observed average radial power spectra (dashed lines) and seeing corrected power spectra (solid lines) of the five data sets from experiment 1.

https://doi.org/10.1017/S0252921100108401 Published online by Cambridge University Press

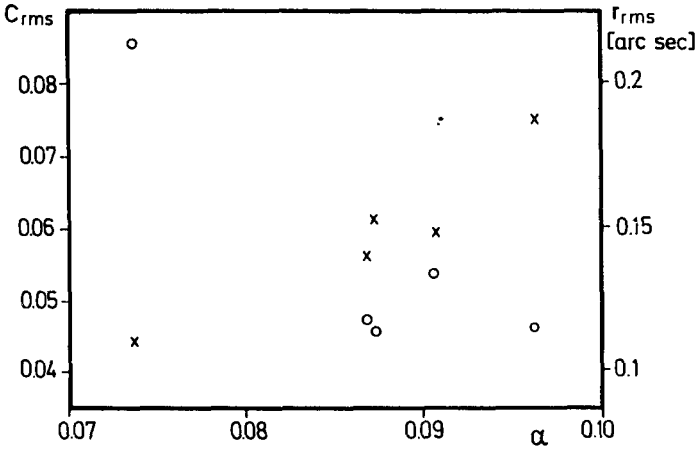

Fig.7. Average rms image contrast (X) and rms radial image displacement (O) of the five data sets in experiment 1 displayed as a function of the modified FRIED parameter α found with the spectral ratio method.

T A B L E I
experiment 1

data taken at SPO vacuum tower tel. on Sept. 10th, 81

32x32 pixel diode array	
field of view:	6".23
resolution:	0".198/*pix*
exposure time:	5 *ms*
frame rate:	18/*s*
wave length:	444 *nm*

TABLE II

Seeing parameters and contrast values for the five sets of data

Set No.	α	r_o(cm)	Δr_{rms} (arcsec)	observed C_{rms}	compensated C_{rms}
1	o.o963	6.74	o.115	o.o747	o.291
2	o.o873	6.11	o.111	o.o61o	o.275
3	o.o869	6.o8	o.117	o.o558	o.252
4	o.o9o7	6.35	o.134	o.o591	o.262
5	o.o737	5.16	o.214	o.o442	o.285

Δr_{rms} is the rms radial image displacement from average image position

https://doi.org/10.1017/S0252921100108401 Published online by Cambridge University Press

$$P_r(\bar{q}) = \int_0^{2\pi} P(q,\vartheta)\, d\vartheta \qquad (16)$$

The convergence of the compensated spectra (differing by a factor of 1.4 at most; solid lines) as compared to the raw spectra (dashed lines) is noticeable. In Fig. 7, a comparison between the conventional seeing indicators, the observed rms image contrast and rms image motion, is presented. These results are discussed in a greater depth in VON DER LÜHE (1984).

The second experiment was carried out with a larger pixel number and a better resolution (cf. Table III). Again, solar granulation at the center of the solar disk was the observed structure. In Fig. 8 a-d, four sample frames are shown to give an impression of the quality of the data set. Each frame became Fourier transformed; the average power spectrum (Fig. 9) and the average Fourier transforms from 3o and 6o frames were calculated. Again, a flat field run was used to estimate the noise bias in the average power spectrum and eqn. (6) was used to compute the spectral ratio (Fig.1o). The ratio exhibits excellent radial symmetry, which is caused by the isotropic statistics of both seeing (center part) and the granulatory intensity distribution (broad, dark ring). Eqn. (15) was used to calculate the average radial profile of the spectral ratio. The result is shown in Fig.s 11 a and b, for averages of 3o and 6o frames, respectively.

Here, the decrease of the curve about q = o.1 marks the radius of the central, bright region in Fig. 1o and, thus, the relative decay of the average Fourier transforms when compared with the average power spectrum. This decay is consistent with r_o equal to 6 cm. The decrease is followed by a section, where the spectral ratio has a typical value of o.o4 (averages of 3o frames) or o.o26 (averages of 6o frames). This section corresponds to the "dark ring" in Fig.1o and identifies the regions, where speckle interferometry signal is present in the average power spectra. If we assume the gaussian noise model and apply eqn. (9), we would end up with SNR values of 4.5 (3o frames) and 4.9 (6o frames). The improvement in SNR thus may be only marginal. Beyond q= o.4, Fig.s 11 a and b reflect the "chaotic" behaviour of the spectral ratio when SNR is small. In Fig.s 1o and 11, negative values are suppressed.

In Fig. 12, the observed radial spectral ratio is plotted together with the corresponding KORFF modulation transfer function. The latter was used to restore the observed average power spectrum using 3o frames (solid line in Fig.13, the dashed line represents the radial noise spectrum as obtained from a flat field test set). The result of the restoration is shown in Fig.14.

https://doi.org/10.1017/S0252921100108401 Published online by Cambridge University Press

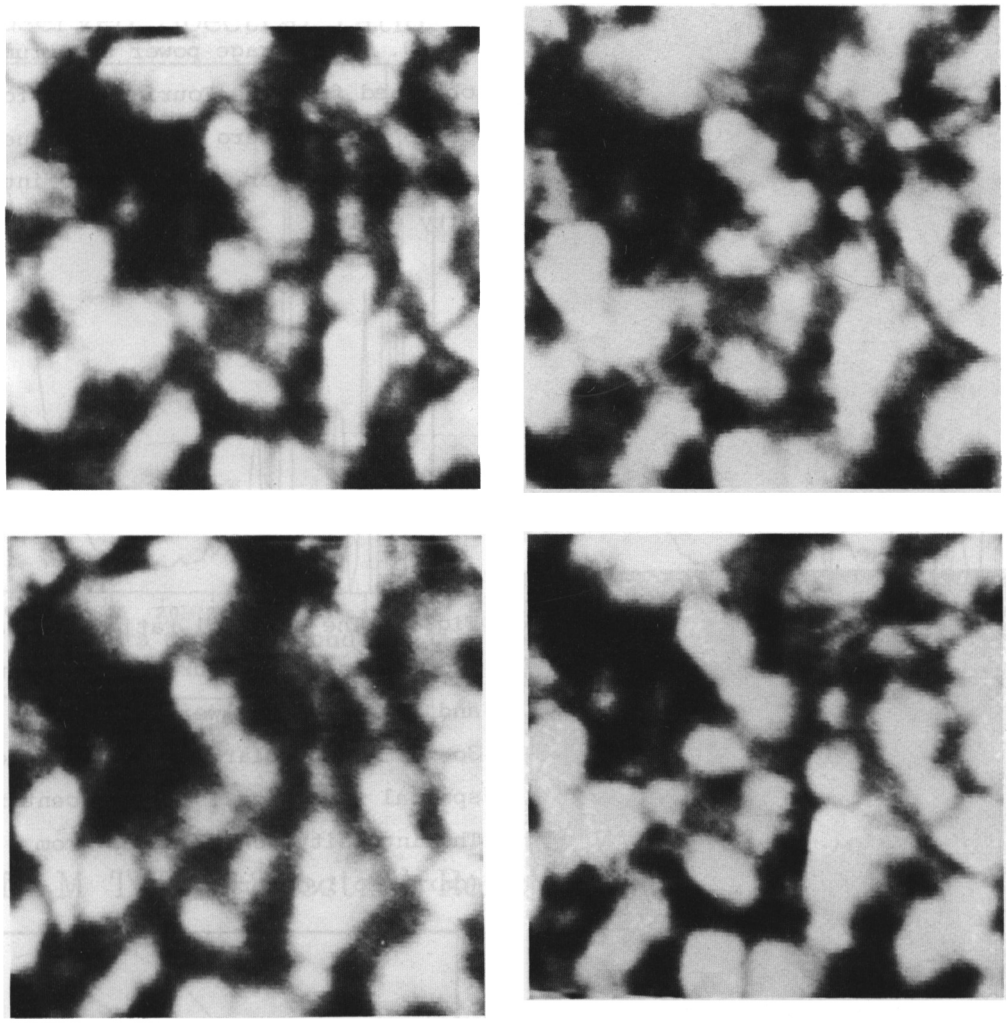

Fig.8. Four sample frames from the data analysed in experiment 2 (see text and TABLE III). The frames have 14" side length.

https://doi.org/10.1017/S0252921100108401 Published online by Cambridge University Press

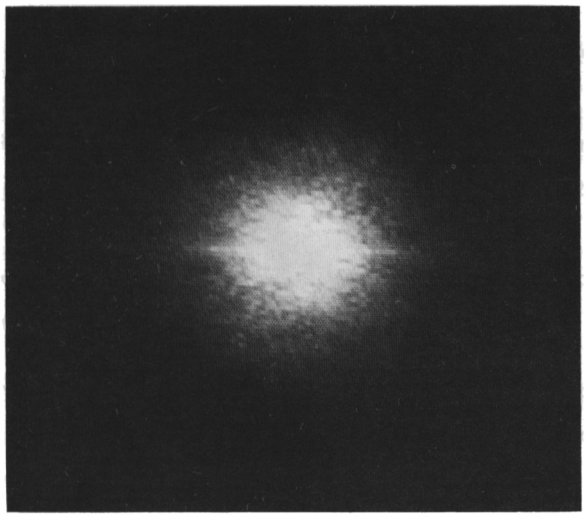

Fig.9. The average power spectrum obtained from the Fourier transforms of 3o frames. Zero spatial frequency is at the center. Logarithmic intensity scale.

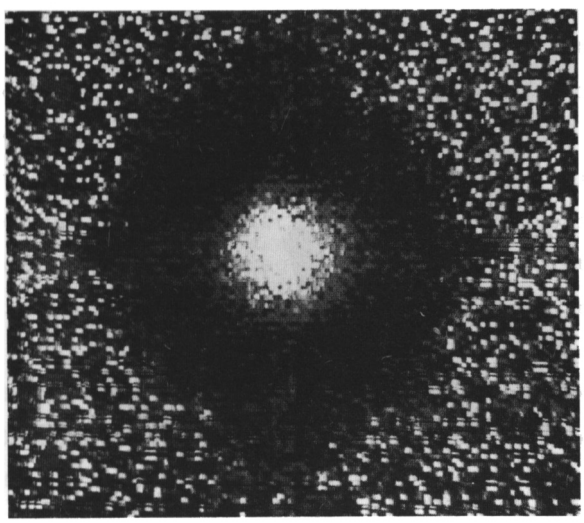

Fig.1o. The spectral ratio calculated from the average Fourier transform and the average power spectrum of 3o frames of solar granulation. Zero spatial frequency is at the center. The intensity scale ranges from o.o (dark) to 1.o (bright).

T A B L E III
experiment 2

data taken at SPO vacuum tower tel. on June 17th, 83

M D A	*128x128 pixel*
field of view:	14".3
resolution:	0".107/*pix*
exposure time:	4 *ms*
frame rate:	0.55 *s/fr*
wave length:	517 *nm*

https://doi.org/10.1017/S0252921100108401 Published online by Cambridge University Press

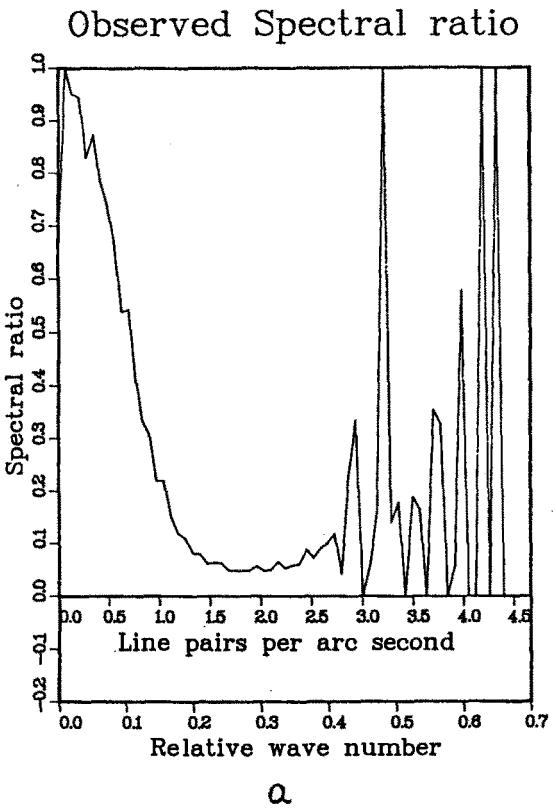

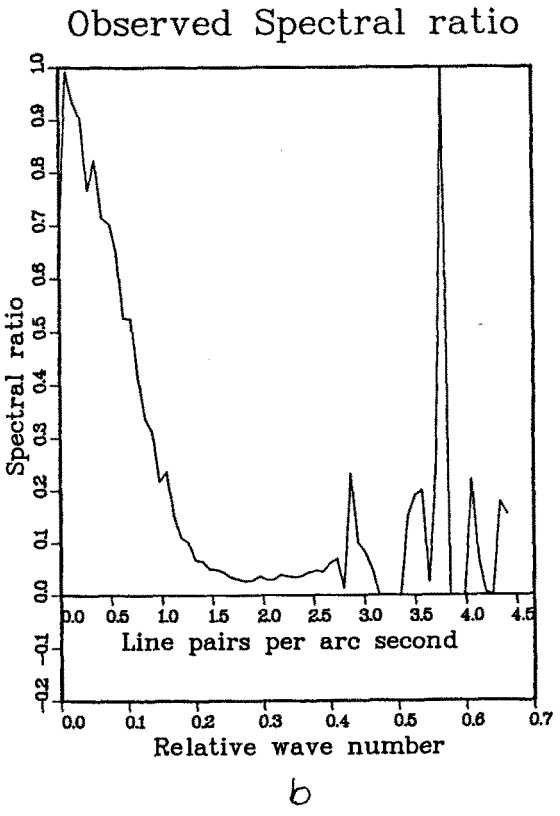

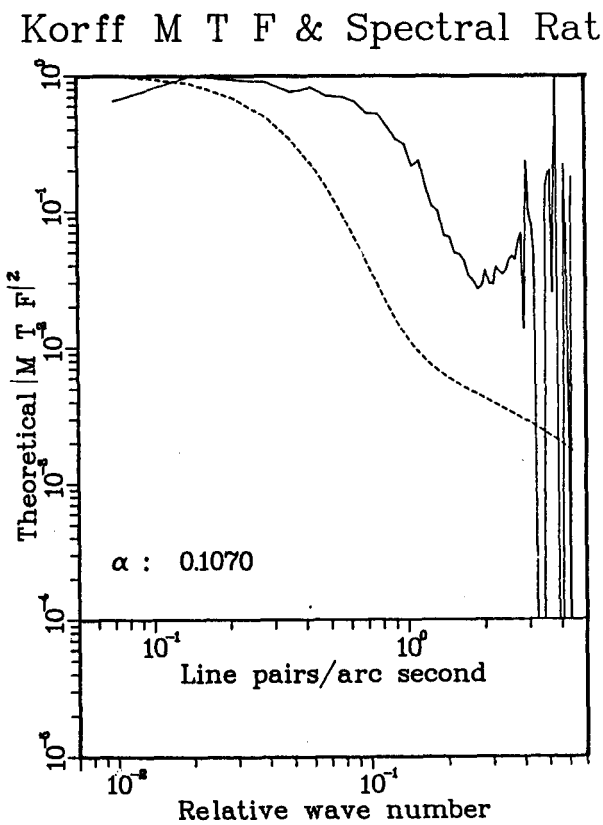

Figs. 11a and b.
The azimuthal average of the 2D spectral ratio. Fig.11a: spectral ratio calculated from averages of 3o frames, Fig.11b: averages of 6o frames. Negative values were set to zero in the plots.

Fig.12. The spectral ratio from Fig.1o (solid line) plotted together with the corresponding KORFF KORFF average MTF^2 (dashed line) in a double log scale.

https://doi.org/10.1017/S0252921100108401 Published online by Cambridge University Press

IV. Experiences and Conclusions

In sect. II, it was explained that in order to obtain theoretical spectral ratios from FRIED's and KORFF's theories, the so-called "short-exposure time" average modulation transfer function (FRIED, 1966) was used. This is justified only, when care has been taken to remove the relative image displacement of each frame of a given data set, i.e. to bring all frames of a time series into registration. Each image shift, described by a vector $\vec{a}$ in image space, causes a factor of $\exp(i\beta q \cdot a)$ in the corresponding Fourier transform (β is a constant). When image shifts are caused by image motion due to seeing, $\vec{a}$ will be a random quantity. The corresponding average Fourier transform would have smaller moduli in comparison with an average Fourier transform that is not affected by image motion.

Thus, the frames were brought into registration by a technique that has been described earlier (VON DER LÜHE, 1983). However, image displacements could only be considered in integer units of pixel lengths in order to avoid loss of high spatial frequency information, so image displacements of fractions of a pixel length remain. The effect is a slightly attenuated average Fourier transform which causes a tendency to underestimate the seeing parameter α and thus to overestimate the effect of seeing in the powerspectrum. A simple model calculation reveals, however, that this effect would be very small at small wave numbers, and can be neglected.

The alternative would have been to use FRIED's 'long-exposure-time" average MTF instead of correcting image motion. But, practically, image motion may be caused by telescope movements as well as seeing, which would change the statistics of the image displacements, so we feel that the procedure described previously is better.

Anisoplanatism may have a similar effect on the average Fourier transform, which we couldn't account for. Qualitatively, anisoplanatism can be separated into image distortion and a spatially variable diameter of the seeing disk. In a simple model, both effects would lead to "crosstalk" between neighouring frequency bins in the Fourier transform of a single frame and thus may attenuate the average transform. We know that, at least, noticeable image distortion is present in the material used for the second experiment. However, reducing the effective size of the field of view by a factor of 0.78 when applying a different apodisation bell did not change the seeing parameter obtained from our analysis at all.

https://doi.org/10.1017/S0252921100108401 Published online by Cambridge University Press

We have presented the theory of a method that allows to obtain an estimate of FRIED's seeing parameter r_o from a set of observations of an arbitrarily structured, astronomical object. Additionally, the method allows to estimate the signal-to-noise ratio of the speckle interferometry signal in the Fourier domain. We comment on the effect of image motion and anisoplanatism to the spectral ratio.

From the experiments, we draw the following conclusions:

- The observed spectral ratios are reasonably explained with spectral ratios modeled with the use of FRIED's (1966) and KORFF's (1973) theories.

- The power spectra, obtained from averages of time series under changing seeing conditions, and restored with a KORFF modulation function using the r_o-estimates from the spectral ratio method, converge (first experiment).

- The noise bias in the spectral ratio in the first experiment can be consistently explained with the presence of a systematic noise component of the Fourier transforms (fixed pattern noise).

- The noise bias in the second experiment can be explained with the presence of a random component in the Fourier transforms.

- When observing solar granulation, we observe signal with a reasonable SNR up to a spatial frequency of 2.7 line pairs/arc second (approx. 2o Mm^{-1}) under good seeing conditions (r_o = 6 cm) with data covering 15..3o seconds of time. As a consequence for image restoration, it should be possible to reconstruct structure with a scale of roughly 1/3 arc seconds in a reasonable time with a 6o cm telescope under these seeing conditions.

References

Aime, C., Ricort, G., Roddier, C., Lago, G.: J. Opt. Soc. Am. 68, 8 (1978)
Dainty, J.C.: Mon. Not. R. Astr. Soc. 169, 631-641 (1974)
Fried, D.L.: Journ Opt. Soc. Am. 56, 1o, 1372-1379 (1966)
Korff, D.: Journ. Opt. Soc. Am. 63, 8, 971-98o (1973)
von der Lühe, O.: Astron. Astrophys. 119, 85-94 (1983)
von der Lühe, O.: Journ. Opt. Soc. Am. A (in press)
Noyes, R.W., Stachnik, R.V., Nisenson, P.: Speckle Image reconstruction of

https://doi.org/10.1017/S0252921100108401 Published online by Cambridge University Press

Solar features. Air Force Geophysics Lab report TR o155, Air Force Systems command, USAF Hanscom AFB, Mass. o1731.

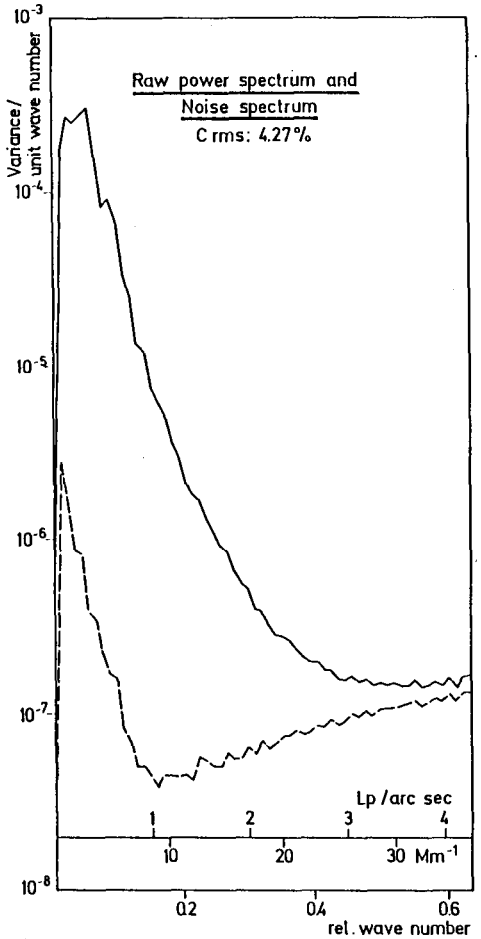

Fig.13. The radial average power spectrum (solid line) and the average noise bias as obtained from a flat field run (dashed line).

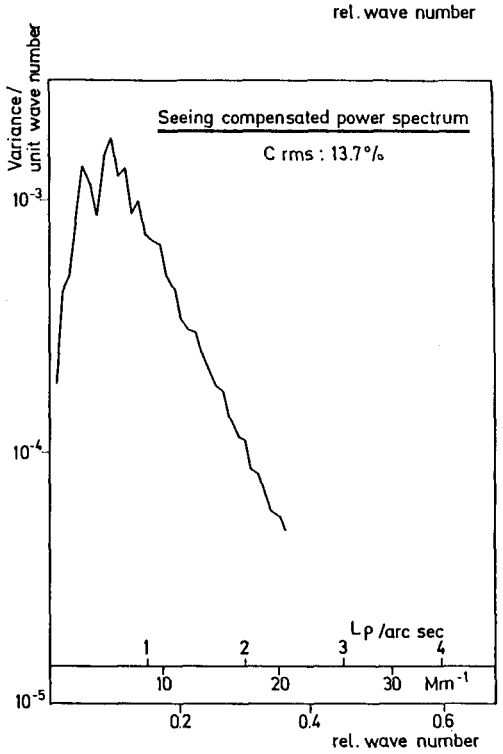

Fig.14. The average power spectrum of Fig. corrected with the KORFF MTF² from Fig.12.

https://doi.org/10.1017/S0252921100108401 Published online by Cambridge University Press